Modelling of Mixing and Simulation of its Effect on Glutamic Acid Fermentation*

B. Mayr[a], E. Nagy[b], P. Horvat[c], and A. Moser[a]**
[a]Technical University of Graz,
Petergasse 12/I, A-8010 Graz, Austria
[b]Research Institute for Chemical Engineering
Hungarian Academy of Sciences
P.O.Box 125, 8201 Veszprém, Hungary
[c]Faculty of Food Technology and Biotechnology,
University of Zagreb
Pierottijeva 6, HR-41000 Zagreb, Croatia

UDC 66.063
Conference paper
Received: August 28, 1992
Accepted: December 20, 1992

This work deals with the hydrodynamic behaviour of bioreactors and its impact on the microbial metabolism. Numerous mixing tests were carried out, using the heat pulse technique and a measurement system containing several sensors. The quantification of the experiments in the batch bioreactors lead to a new approach, the so called "homogeneity-time", which should replace the mixing-time. In order to understand more about the flow behaviour in the bioreactors, the flow models proved to be a successful instrument. The modelling was accomplished with macroscopic mechanistic flow models on the basis of the tanks-in-series approach. A procedure for the optimization of the adjustable model parameters was developed. A new hydrodynamic Scale-Up method for a three stage stirred tank was presented. This provided the basis for further work on a combination model including both hydrodynamic and kinetic phenomena. As a first case study influences of the mixing behaviour on the control of the pH-value were examined for a glutamic-acid fermentation.

Key words:
Bioprocess, simulation, structured model, mixing, kinetic

Introduction

Successful scale-up and the definition of the optimal operational conditions of batch bioprocesses are – inspite of numerous investigations – still a difficult problem, because the optimal process variables are usually evaluated in relatively small lab-scale bioreactors. These lab-scale fermentors are assumed to be ideally mixed or pseudo-homogeneous[1], since the corresponding time constants of the mixing process are sufficiently small compared to the ones of the microbial and mass-transport processes.

During scale-up the time constants of the mixing process grow significantly. Bajpai and Reuss[2] state that "In order to understand the influence of the geometry and scale of operation, the distributions of mass and energy should be coupled with kinetic processes in bioreactors". A few years earlier Oosterhuis[3] wrote in his thesis that "Basically a scale-up problem exists, when there is a transport of heat, mass or momentum transfer in a system". The bioreactor can not be assumed to be pseudohomogeneous any more and interactions between mixing-, microbial- and transport-processes occur. This becomes especially important in the case of viscous fermentation broths. As a consequence the optimal process variables can not be matched. The influence of these changes on the yield of the bioprocess can only be quantitavely evaluated by combined structured-mixing-, formal-kinetic and mass-transfer models. These combined structured models can also be used to simulate operating trouble such as an interrupting in strirring or aerating.

So far theoretical background has been set up, but suitable structured mixing models with parameters adjusted on the basis of reliable measurements in industrial bioreactors are still missing. In the case of structured mixing models Jury[4] started this work for bubble-column and airlift-bioreactors. Anyhow the verification of the combined structured models can only be achieved in large scale industrial bioreactors.

Material and methods

The mixing-experiments were carried in stirred tank bioreactors equipped with three Rushton turbines in scales of 0.12, 2.5 and 65 m^3.

The tanks are operating batchwise and the mixing behaviour was determined by use of the heat pulse technique[4,5,6,7] in case of the smaller tanks. For the largest fermentor (65 m^3) the pH-transient method was applied.

*Workshop on Bioprocess Simulation in Practice, Graz 14, 1992
**Author to whom correspondence should be adressed

Table 1 – *Technical features of the bioreactors*

Synonym	Tank volume	Stirrer	Turbine diameter	Max. power	Tank diameter	h_l/d	Liquid volume
–	m^3	–	m	kW	m	–	m^3
STR-3-S	0.15	3 Rushton	0.21	3	0.40	2.3	0.12
STR-3-M	3.2	3 Rushton	0.51	26	1.18	2.3	2.5
STR-3-L	90	3 Rushton	1.42	420	3.50	2.0	65

Table 2 – *Experimental conditions*

Fermentor	Stirrer revolutions	Aeration rate	Power input	Medium	Density	Viscosity
–	rps	$m^3\ h^{-1}$	kW	–	$kg\ m^{-3}$	Pa·s
STR-3-S	0.83; 1.67; 3.3; 5; 6.67	0; 2.4; 4.2; 6; 9	0.02–3	tapwater; glycerolwater	998.3; 1218.1	0.001; 0.18
STR-3-M	1; 1.67; 2.5; 3.3; 4.17	0; 40; 70; 100; 150; 200	0.26–26	tapwater; glycerolwater; ferm. br.	998.3; 1218.1; 1050	0.001; 0.18; 0.04
STR-3-L	0.5; 1.1; 1.4	0; 2000	24–400	fermentation broth	1050	0.7

Fermentors

Bioreactors with technical features given in table 1 were examined.

All bioreactors are supplied with 4 baffles, geometrical details for the tanks STR-3-S and STR-3-M are given elsewhere[6]. The geometrical details for the setup STR-3-L are illustrated in figure 1 and described in tables 1 and 2.

Measurements

In case of STR-3-S and STR-3-M the heat pulse method was used to investigate the flow properties. Six PT-100 sensors were positioned in the bioreactors[6] and their responses to the temperature pulse were recorded by means of an electronic interface connected to a personal computer.

For the largest fermentor (STR-3-L) the pH-transient method was utilized. The pulse of acid or base was poured to the liquid surface near the stirrer shaft.

One probe with a response time (10 to 90%) of approximately 0.9 s recorded the distribution of the tracer.

The experimental conditions for all tests are given in table 2.

All combinations of stirrer rotations, aeration rates and viscosities were tested.

The temperature was kept in the range between 22 °C to 26 °C.

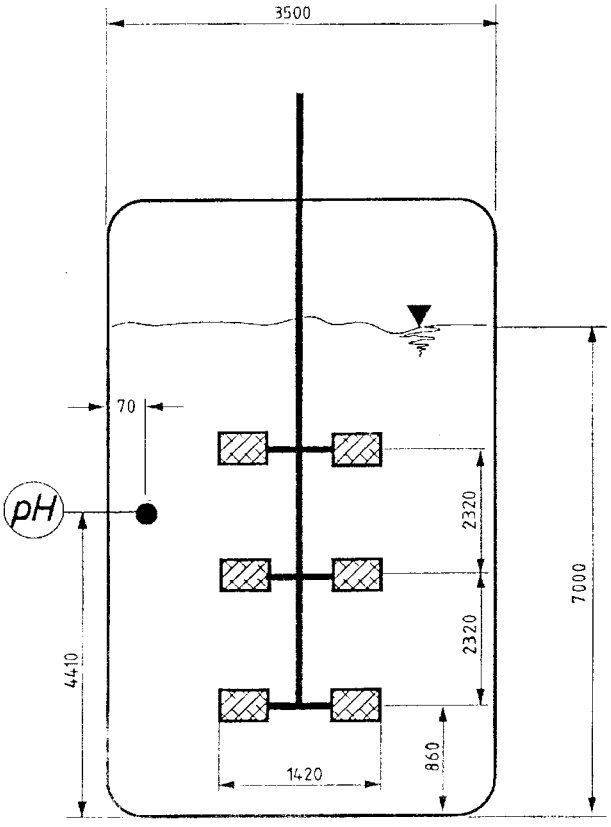

Fig. 1 – *Geometrical dimensions and sensor position in the stirred tank bioreactor STR-3-L with 65 m^3 liquid volume*

Results and discussion

Quantification of the mixing behaviour

The mixing behaviour of batch reactors is usually investigated by the application of a pulse of tracer, commonly a Dirac pulse function is used[8]. The distribution of the tracer in the tank is recorded by one or more sensors. The pulse should show, on the one hand, a behaviour close to a Dirac function and on the other hand should not disturb the flow structure. For these reasons the design of the pulse injection system is extremly important. After several tests the proper pulse application system for a stirred tank was defined as a sparger right below the middle turbine. Details concerning the hydrodynamic and geomatrical design were given in previous works[9,10].

In Fig. 2 a typical batch-mixing experiment is presented.

As soon as it was possible to run the experiments reproducible it became obvious that the widely used mixing-time gave inexact resulst, because the times varied with the location of the pulse input as well as with the position of the sensors in the tank[6,11]. Anyhow a quantification of a time when the mixing process is approaching the ideal state is desireable, since this gives a quick first impressions of the rate of mixing. If this time is faster than all other process relevant time-constants, the mixing will not be limiting and the system is considered to be pseudohomogeneous[1]. We defined this new "homogeneity-time" in the way demonstrated in Fig. 2 and Fig. 3. First the ideal response curve M(t) is calculated according to eq.(1), then all individual response curves T_i are related on this curve (Fig. 2).

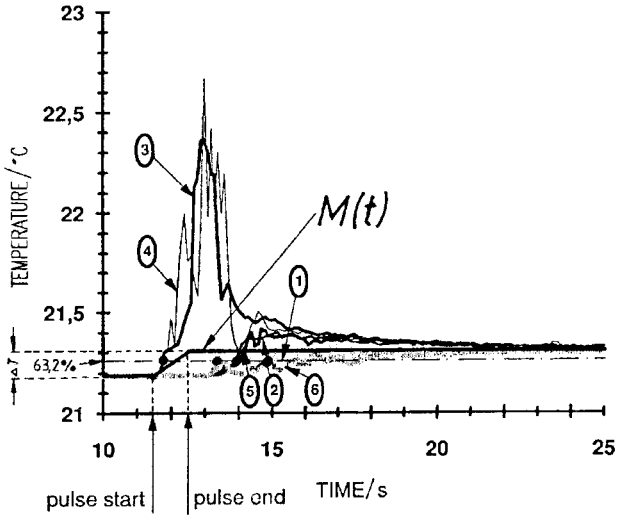

Fig. 2 – *System response of STR-3-M bioreactor to temperature pulse. The numbers specify the individual sensor responses[6]. Experimental conditions:*
Q_G=40 m³/h, n=100 rpm, tap water

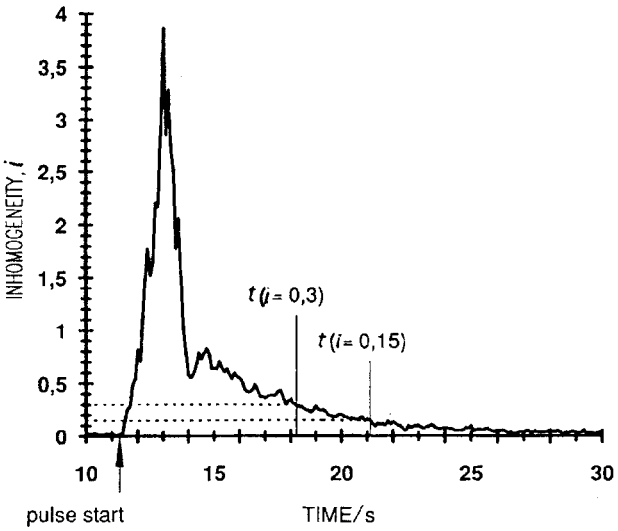

Fig. 3 – *Inhomogeneity curve and homogeneity times obtained from system response shown in Fig. 2*

$$M(t) = T_S, \quad t < t_{PS}$$
$$M(t) = f(t), \quad t_{PS} < t < t_{PE}$$
$$M(t) = T_E, \quad t > t_{PS} \qquad (1)$$

$$f(t) = \frac{c_{P,P}}{c_{P,S}} T_P - \frac{\frac{c_{P,P}}{c_{P,S}} T_P - T_S}{\left[1 + \frac{Q_P}{V_S}(t - t_{PS})\right]^{\rho_P/\rho_S}}$$

The mean of all absolute differences is divided by the total temperature increase ΔT. The resulting so called "inhomogeneity-curve i(t)" is plotted in Fig. 3. This curve represents the time dependency of the inhomogeneity of the whole reactor system if all significant compartments are measured. The homogeneity-time is defined as the time elapsed from pulse injection until the inhomogeneity function i(t) drops below a certain conventional value. Because of the definition the homogeneity-time for i = 0.15 is equivalent to a mixing-time for 85%' degree of mixing. The homogeneity-time defined in this way should replace the widely used mixing-time as the criterion for the mixing rate of bioreactors if more than one sensor is used. Another advantage of this method is that the noise in the signal nearly drops out in this case. This quantification method was discussed in detail in a previous paper[6].

Two other measures proved to be significant for the batch mixing process. The first one is the time-constant for each sensor signal, in other words the time from pulse injection until the signal reaches 63.2% of the end temperature for the first time (indicated in Fig. 2). The differences between these times give good approximates for the transit times of the flow between the sensor locations. The second is the maximum of the inhomogeneity-curve, because this number is related to the size

of the ideally mixed volume around the middle turbine, where the pulse is injected.

Additional information about these two quantification methods can be found in another article[12].

Mixing model

Mixing models on basis of the tanks-in-series concept have been used for two main reasons:

– the first one is that it would be possible to set up flow models for the most common bioreactors. This has been so far for airlift and bubble column fermentors[4], for deep-jet-fermentors[13,14], but also for stirred tanks[2,4,17–24].

– the second argument is that corresponding mathematical models consist of a reasonable amount of coupled first order differential equations, usually not exceeding 50. This is important, since it will be possible to superpose a kinetic model later on.

As it becomes clear from Fig. 4, the compartments are connected to each other in a way similar to the real macrospopic flow pattern, as it is presented here for the case of stirred tanks.

A few preconditions for the use of these kinds of models remain:

– the macroscopic flow pattern must be qualitatively known

– reliable model parameters can only be obtained if a large database is available

The parameter-estimation process with optimization in case of the stirred tank experiments is illustrated in Fig. 5.

The first step is the calculation of the significant criteria of the test. These criteria were already introduced:

– homogeneity-time

– time constants

– maximum of the inhomogeneity-curve

In the second step initial values for the adjustable model parameters are selected. This is of major importance since with these kinds of mathematical models several local optima might occur. In order to detect the global optimum the initial point must already be in a proper region. Therefore the model was tested about 1000 times with different parameter combinations of the adjustable model parameters. The above mentioned criteria were calculated for the model responses as well. The measured results were compared to the stored simulated values and the parameter combination with the smallest absolut deviation was selected as the starting point.

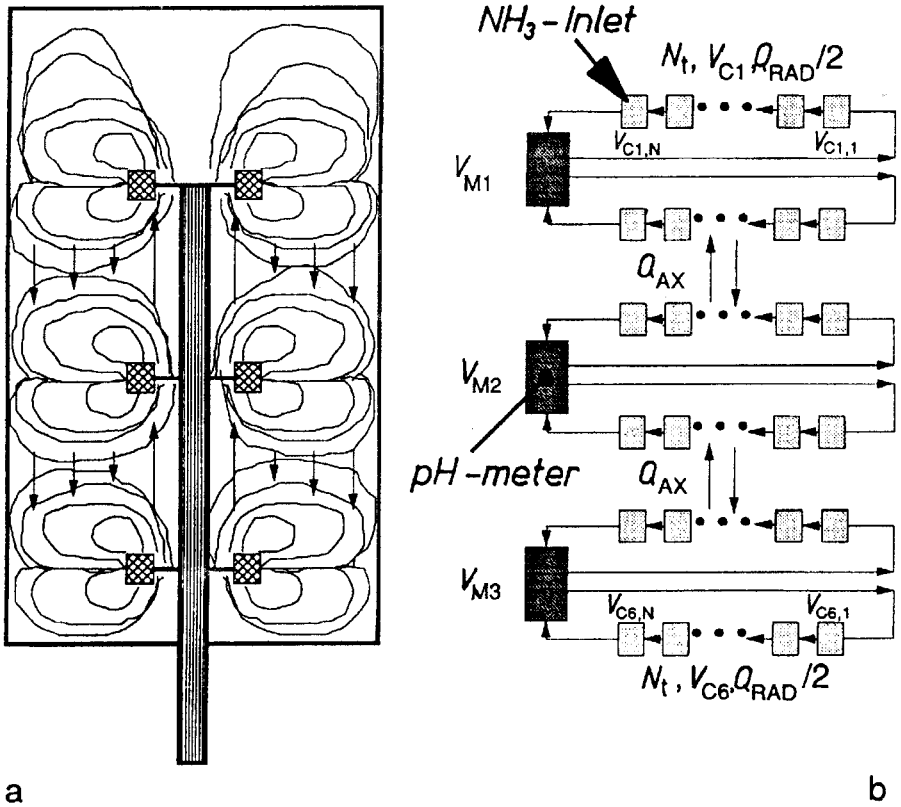

Fig. 4 – *Macroscopic flow pattern (a) and physical mixing model (b) for stirred tank bioreactor equipped with three Rushton turbines* $V_{M1} = V_{M2} = V_{M3} = V_M/3$, $V_{C_{ij}} = V_C/(6 \cdot N)$

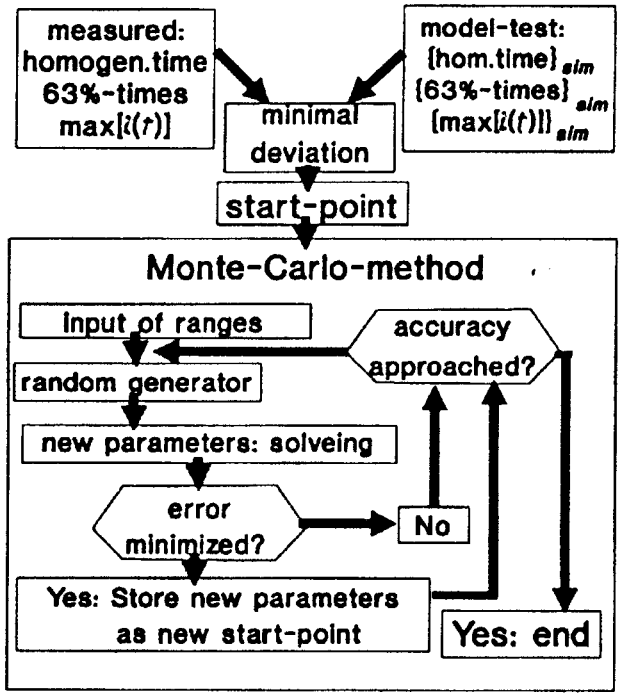

Fig. 5 – *Flowchart of the parameter estimation procedure with Monte-Carlo optimization*

The Monte-Carlo method is started and continues as long as refinements in the adjustable model parameters lead to a reduction of the error, which is the objective function for the optimization process. The error is defined according to eq. (2).

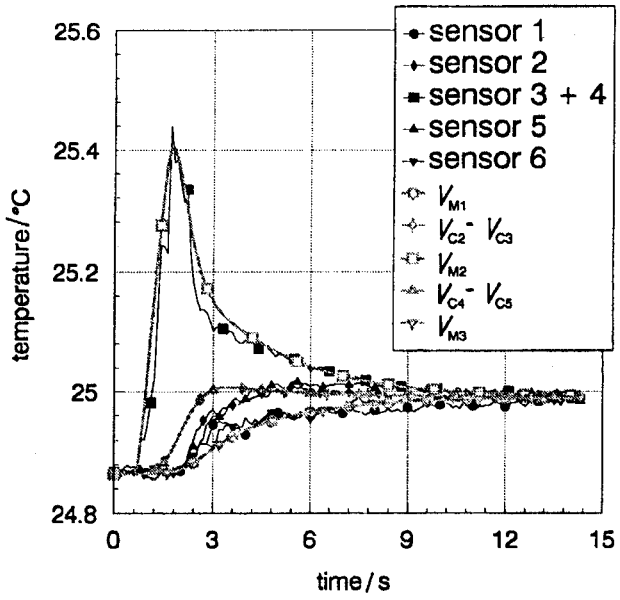

Fig. 6 – *Measured and simulated response functions for STR-3-M setup in case of a central pulse injection*
Experimental conditions:
$n=150$ *rpm*, $Q_G=100\ m^3\ h^{-1}$, $\eta=0.18$ *Pa s*
Model Parameters:
$V_M/V_{tot}=0.21$, $t_{c,RAD}=2.05$, $t_{c,AX}=9.15$ *s*, $N_t=3$

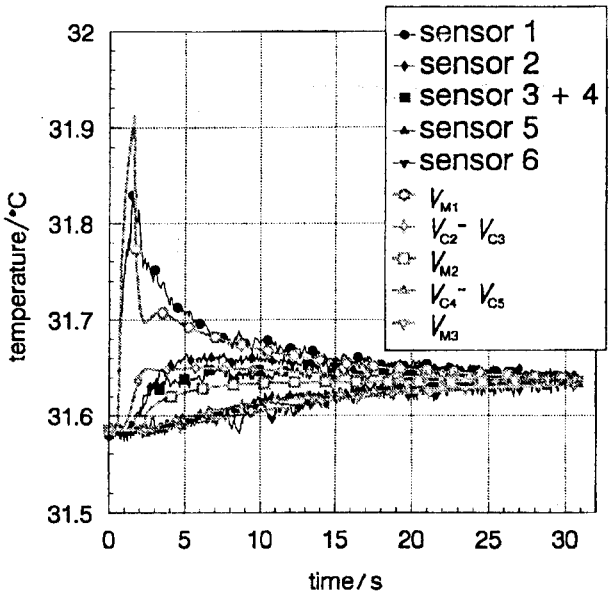

Fig. 7 – *Measured and simulated response functions for the STR-3-M bioreactor, pulse poured onto the surface. Experimental conditions and model parametres are identical to Fig. 4.*

$$error=\frac{100}{2\cdot N_p}\sum_{j=1}^{N_p}\left\{|i_m(t)-i_{sim}(t)|+\frac{\frac{1}{N_k}\sum_{i=1}^{N_k}|T_{i,m}-T_{i,sim}|}{\Delta T}\right\}[\%] \quad (2)$$

Figs. 6 and 7 show the agreement between simulated and measured curves for experiments carried out in the STR-3-M tank. The experimental conditions as well as the related model parameters are listed in the captions.

One of the best methods to test the mixing-model and the experimental setup is an alternation of the pulse input location while all other experimental conditions are fixed, since the real flow pattern should not be influenced by this change. The chosen models as well as the mathematical solutions were tested by means of two different pulse input locations. The result of these investigations are illustrated in Fig. 6 for pulse injection in the center of the tank, i.e. close below the middle stirrer, and in Fig. 7 for the conventional pulse application to the surface.

The model parameters are optimized only in case of Fig. 6. The fit of the model is in range of the turbulent temperature fluctuations for the sensors in the stirred volumes, significant deviations appear only for the response functions in the transient regions (cascades) in the first part of the experiment, i.e. between 1.5 s and 4.5 s. Basically the simulated curves fit well the measured data.

Looking at Fig. 7, with identical experimental conditions (except for the pulse input location) and identical adjustable parameters the following conclusion can be drawn: This model predicts the flow

pattern correctly in respect to time constants of all sensors as well as on the homogeneity-time which is about 2.5 times longer for a top-pulse application. Also the maxima at the beginning of the experimens are predicted correctly[12].

Hydrodynamic scale-up

After the optimization for all measurements in the stirred tank bioreactor have been carried out, the scale-up of the hydrodynamic flow behaviour remains. Mixing measurements are available as listed in table 2 with liquid volumes of 0.12, 2.5 and 65 m^3, the viscosity lies in the range from 0.001 to 0.7 Pa·s. The proposed scale-up concept tries to derive mathematical correlations between the four adjustable mixing model parameters (V_M/V_{tot}, N_t, $t_{c,RAD}$, $t_{c,AX}$) and the four experimental variables (n, Q_G, λ, η). The stirrer revolutions and the gas flow rate are transformed into dimensionless Froude numbers (Fr_S, Fr_A).

The simpliest relation is obtained for the backmixing parameter N, which is kept at a value of 4, since no clear dependences were detected.

$$N_{t\,calc} = 4 \qquad (3)$$

In order to visualize the agreement between this relation and the values resulting from the parameter estimation process, the results are illustrated for the case of the STR-3-L configuration in Fig. 8.

In case of the radial circulation time a relation cited in literature[2] for a Rushton turbine is utilized.

$$t_{c,RAD,calc} = 1/n \cdot 0.76 \cdot (h_l/d_t)^{0.6} \cdot (d_t/d_i)^{2.7} \qquad (4)$$

Fig. 9 shows the calculated values for $t_{c,RAD}$ (eq.4), but also the optimized ones. The values calculated according to eq. (4) are always close to the values resulting from the optimization process. This is in fact a strong hint that the chosen mixing model reflects the real flow structure in the tank correctly.

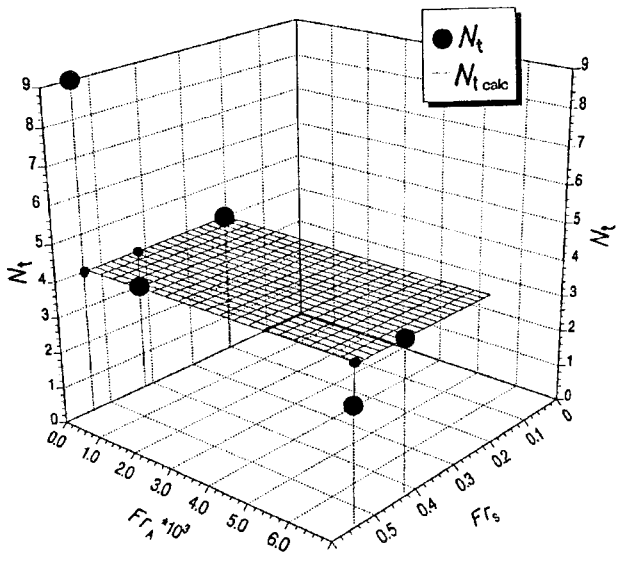

Fig. 8 — *Comparison of the model parameter N_t (as a result of the parameter estimation process) to the value of $N_{t\,calc}$ calculated acc. to eq. (3). STR-3-L tank, η = 0.7 Pa·s*

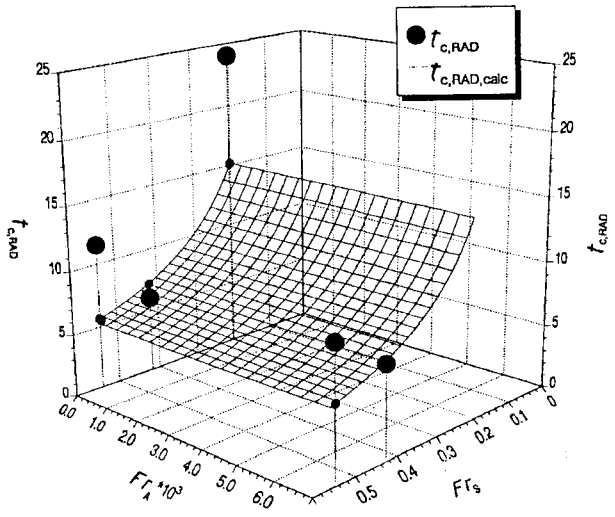

Fig. 9 — *Model parameter $t_{c,RAD}$ as a function of the Froude numbers for stirring and aeration in case of STR-3-L configuration. Values of $t_{c,RAD,calc}$ [acc. to eq. (4)] are plotted as well, η = 0.7 Pa · s*

The remaining two model parameters ($t_{c,AX}$, V_M/V_{tot}) have been found to be strongly dependent on all experimental variables. Therefore a slightly more complicated mathematical expression is used in these cases.

It is important to notice that the given correlations are only valid in the examined range (Fig. 10) which is indicated crosshatched, an extrapolation is not recommended.

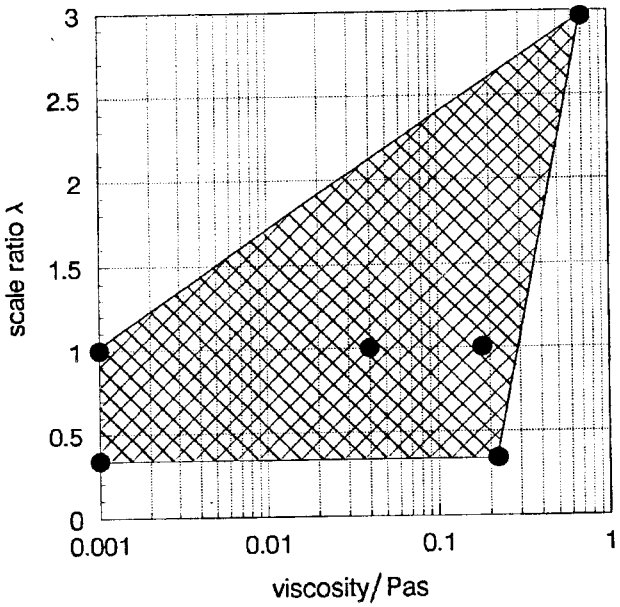

Fig. 10 — *Validity boundaries for viscosity and scale ratio: valid range is marked crosshatched*

The equation for the axial circulation time ($t_{c,AX}$) includes all experimental variables. This adjustable parameter has been found to be stronger dependent on the aeration rate that on the stirrer revolutions, therefore this parameter is related with the second power on the aeration Froude number and linearly on the stirrer Froude number. A surface equation [acc. to eq. (5)] is fitted to all axial circulation times for all examined combinations of viscosity and scale ratio. The mathematical surface regression method of the 3D-Visions-Corporation software package "GRAFTOOL" is used.

$$t_{c,AX,calc} = a_{00} + a_{01} \cdot Fr_A \cdot 10^3 + a_{02} \cdot (Fr_A \cdot 10^3)^2 + a_{10} \cdot Fr_S + a_{11} \cdot Fr_S \cdot Fr_A \cdot 10^3 + a_{12} \cdot Fr_S \cdot (Fr_A \cdot 10^3)^2 \quad (5)$$

The coefficients in eq. (5) include the dependence on viscosity as well as on scale ratio (eq. 6–12). These equations are obtained by use of the mentioned surface regression method. As an example one of these surface equations (a_{00}) is illustrated in a 3D-plot (Fig. 11).

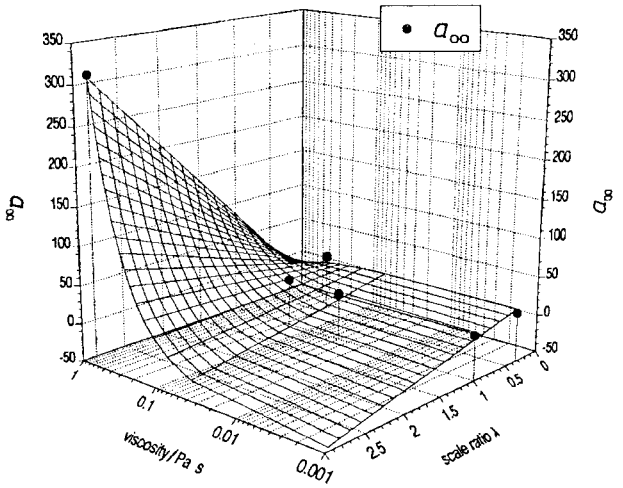

Fig. 11 – *Surface equation coefficient a_{00} for the model parameter $t_{c,AX}$ in dependence on scale ratio and viscosity. Eq. (6) describes the plotted surface.*

Equations for the regression coefficients:

$$a_{00} = 29.07 - 25.08 \cdot \lambda - 106.6 \cdot \eta + 207.6 \cdot \eta \cdot \lambda \quad (6)$$

$$a_{01} = -4.089 + 3.958 \cdot \lambda + 1.333 \cdot \eta - 18.28 \cdot \eta \cdot \lambda \quad (7)$$

$$a_{02} = -0.0098 - 0.0027 \cdot \lambda + 1.911 \cdot \eta - 0.972 \cdot \eta \cdot \lambda \quad (8)$$

$$a_{10} = -26.88 + 31.97 \cdot \lambda + 148.7 \cdot \eta - 268.1 \cdot \eta \cdot \lambda \quad (9)$$

$$a_{11} = 5.678 - 6.343 \cdot \lambda - 20.65 \cdot \eta + 35.26 \cdot \eta \cdot \lambda \quad (10)$$

$$a_{12} = -0.190 + 0.213 \cdot \lambda - 0.242 \cdot \eta - 0.176 \cdot \eta \cdot \lambda \quad (12)$$

The goodness of the value for $t_{c,AX,calc}$ calculated acc. to eq. (5) is demonstrated in Fig. 12, experimental conditions are given in the captions.

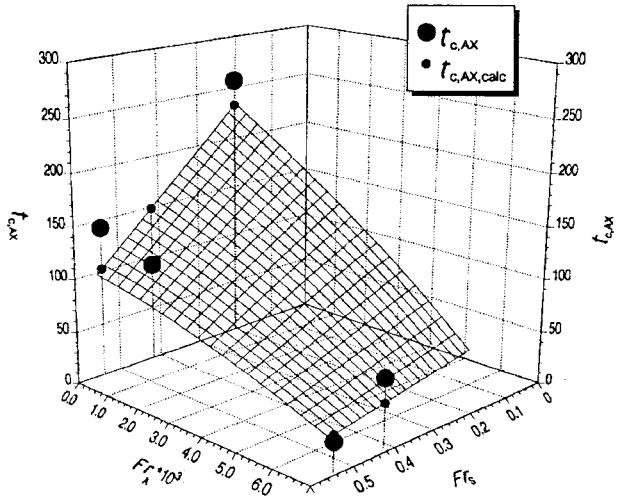

Fig. 12 – *Adequacy of values for $t_{c,AX,calc}$ calculated acc. to eq. (5) in comparison to the values resulting from the parameter estimation procedure. STR-3-L configuration η=0.7 Pa·s*

The correlation for the ideally mixed compartment (V_M/V_{tot}) is also dependent on all experimental variables. The same procedure as for the determination of the axial circulation time is applied again, except that the parameter $(V_M/V_{tot})_{calc}$ is related with the second power on Fr_S and linearly on Fr_A in contradiction to $t_{c,AX,calc}$.

$$(V_M/V_{tot})_{calc} = b_{00} + b_{01} \cdot Fr_A \cdot 10^3 + b_{10} \cdot Fr_S + b_{11} \cdot Fr_S \cdot Fr_A \cdot 10^3 + b_{20} \cdot (Fr_S)^2 + b_{21} \cdot (Fr_S)^2 \cdot Fr_A \cdot 10^3 \quad (13)$$

Again, the validity boundaries should not be exceeded and are indicated crosshatched in Fig. 10.

Equations for the regression coefficients:

$$b_{00} = 0.166 - 0.308 \cdot \lambda + 1.428 \cdot \eta - 0.134 \cdot \eta \cdot \lambda \quad (14)$$

$$b_{01} = -0.013 + 0.044 \cdot \lambda - 0.082 \cdot \eta - 0.026 \cdot \eta \cdot \lambda \quad (15)$$

$$b_{10} = -0.414 + 1.381 \cdot \lambda - 2.594 \cdot \eta - 0.826 \cdot \eta \cdot \lambda \quad (16)$$

$$b_{11} = 0.098 - 0.240 \cdot \lambda + 0.262 \cdot \eta + 0.195 \cdot \eta \cdot \lambda \quad (17)$$

$$b_{20} = 0.863 - 1.301 \cdot \lambda + 1.311 \cdot \eta + 0.959 \cdot \eta \cdot \lambda \quad (18)$$

$$b_{21} = -0.176 + 0.255 \cdot \lambda + 0.082 \cdot \eta - 0.296 \cdot \eta \cdot \lambda \quad (19)$$

The adequacy of eq. (13) for $(V_M/V_{tot})_{calc}$ is demonstrated in Fig. 13 for the largest fermentor, the experimental conditions are listed in the captions. The agreement in the smaller volumes is even better, but demonstrated elsewhere[12,16].

A closer description of the proposed scale-up concept will be given in an article which is in preparation[16].

Integrated bioprocess scale-up

So far only the hydrodynamic scale-up has been discussed. Anyhow, the "real" scale-up criteria for a bioprocess are product yield and product quality. It is important to state that usually the scale-

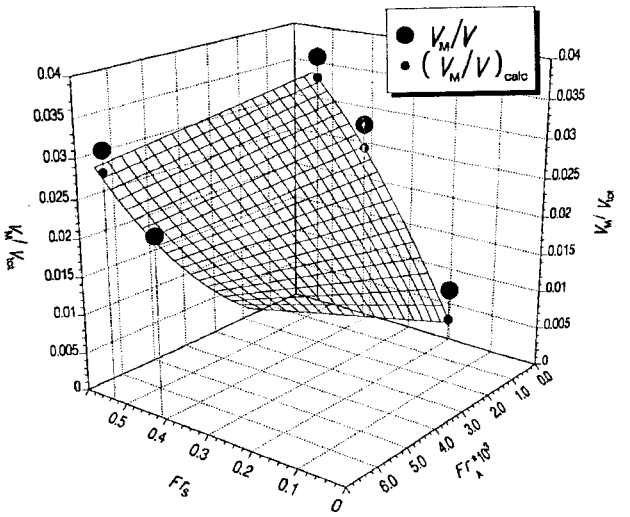

Fig. 13 – *V_M/V_{tot} in function of Froude numbers for stirring and aeration in STR-3-L system, also the goodness of the calculated parameter [acc. to eq. (13)] is demonstrated, η=0.7 Pa·s*

up problem in pharmaceutical industry is not to build a new and larger bioreactor for a certain product, but generally the problem is to scale-up the process by making use of existing bioreactors. In other words a new organism shownig better economics in lab-scale must be adapted to the large bioreactors.

Until nowdays several screening and optimization steps are necessary[1] (Fig. 14), therefore this scale-up procedure is extremly expensive and also takes a long time. For this reason a lot of money is wasted if a process shows a scale-up limitation. This is quite often the case with the oxygen supply.

The aim of the integrated structured model approach presented here is to provide a tool which is capable to predict such limitations already after the first screening step in lab-scale. Of course, the interactions must be quantified, among those are pH- and shear-sensitivity and oxygen uptake.

In a first effort the influence of the mixing on a production of glutamic acid from sugar was investigated. The kinetics of this fermentation is very complex and so far not examined in detail[26,28,29]. The fermentations have been carried out in a so called "perfect bioreactor"[1,27], therefore the mass transfer processes (oxygen absorption and CO_2-desorption) are much faster than the bioreaction. Several unstructured kinetic models have been fitted to the measured concentration data. It turned out that the best model is a "product repression type" kinetic and this model was used in the following studies of the integrated process model. The kinetic equations are the following:

$$-\frac{dC_S}{dt} = \frac{\mu \cdot C_X}{Y_{XS}} + \frac{r_P}{Y_{SP}} \tag{20}$$

$$\frac{dC_X}{dt} = \mu \cdot C_X \tag{21}$$

$$\frac{dC_P}{dt} = r_P = a_P \cdot C_X^2 \tag{22}$$

$$\mu = \frac{\mu_{max}}{C_S + K_S\left(1 + \frac{C_P}{K_P}\right)} \tag{23}$$

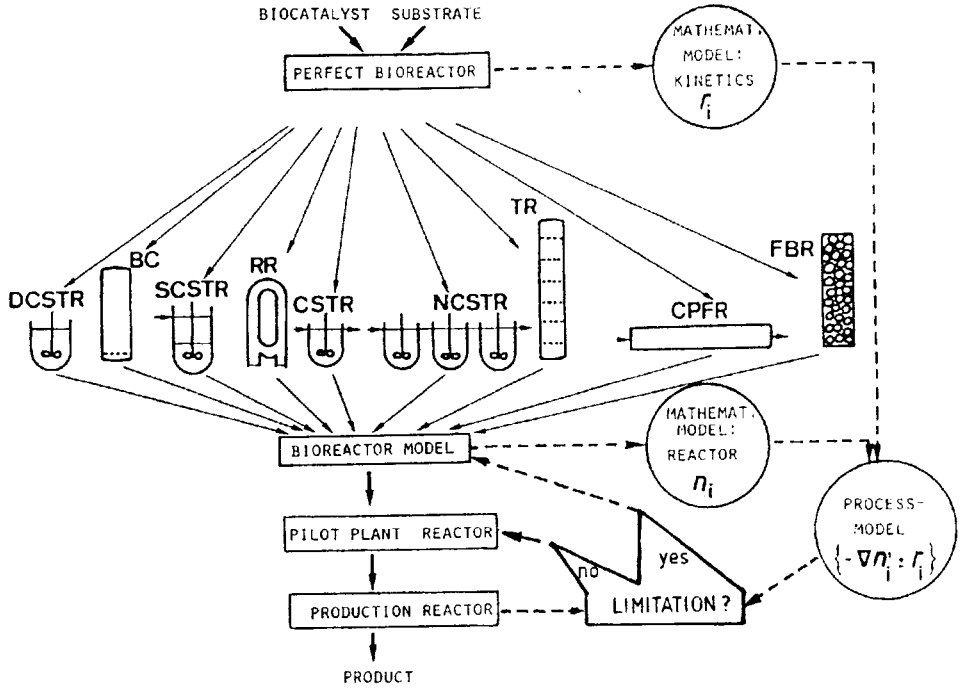

Fig. 14 – *Summary diagram of work flow in the systematic development of a bioprocess (adapted from Moser[1])*

The model does not include any dependence on the biotin concentration, which is an essential factor for the secretion of glutamic acid. Further refinements of the model in respect to this influence will be undertaken.

The calculated data, obtained by a numerical solution of the system of differential equation presented above (eq. 20–23), are fitted to the measured ones. The kinetical model uses four adjustable parameters μ_{max}, K_S, K_P and α_P.

Their numerical values were obtained by means of a parameters estimation method which makes use of a non-linear regression[25].

The mixing of a batch fermentor can only affect a fermentation if internal or external disturbances occur. In order to keep the pH-value constant during the glutamic acid fermentation NH_4OH-solution has to be added continuously. At the beginning of this fermentation the puffer capacity of the broth is low due to the small amount of product. For this reasons an insufficient regulation of the dosage of base results in significant fluctuations in the pH-value and consequently causes an negative effect on the whole fermentation. Therefore the effect of the mixing properties on the regulation (pH-dosage pump capacity, sensitivity of the pH control) of the pH-value was chosen as an external disturbance effect.

For the proposed integrated model the physical mixing model ilustrated in Fig. 4 was selected and combined with the presented kinetic model (eq. 20–23). The concentration of four components, i.e. biomass, substrate, product and ammoniac, have to be calculated. For an arbitrary compartment of the mixing model the following differential equations have to be solved:

$$V_i \frac{dC_{S_i}}{dt} = Q_{RAD}\,(C_{S_{i-1}} - C_{S_i}) - \frac{\mu \cdot C_{X_i}}{Y_{XS}} - \frac{\alpha_P \cdot C_{X_i}^2}{Y_{SP}} \quad (24)$$

$$V_i \frac{dC_{X_i}}{dt} = Q_{RAD}\,(C_{X_{i-1}} - C_{X_i}) + \mu \cdot C_{X_i} \quad (25)$$

$$V_i \frac{dC_{P_i}}{dt} = Q_{RAD}\,(C_{P_{i-1}} - C_{P_i}) + \alpha_P \cdot C_{X_i}^2 \quad (26)$$

$$V_i \frac{dC_{(NH_4OH)_i}}{dt} = Q_{RAD}\,(C_{(NH_4OH)_{i-1}} - C_{(NH_4OH)_i}) \quad (27)$$

Fig. 4 shows the physical mixing model and the locations of NH_3-inlet and pH-meter. The system of differential equations is solved with the Runge-Kutta-Fehlberg integration method.

The adjustable mixing model parameters were taken for a fermentor with 2.5 m^3 liquid volume (λ=1, STR-3-M) and a liquid viscosity (η) of 0.15 Pa·s, with 150 stirrer revolutions per minute (Fr_S=0.6) and an aeration rate of 0.031 $m^3\,s^{-1}$ (Fr_A=0.006).

Typical results for two switching times are presented in Fig. 15.

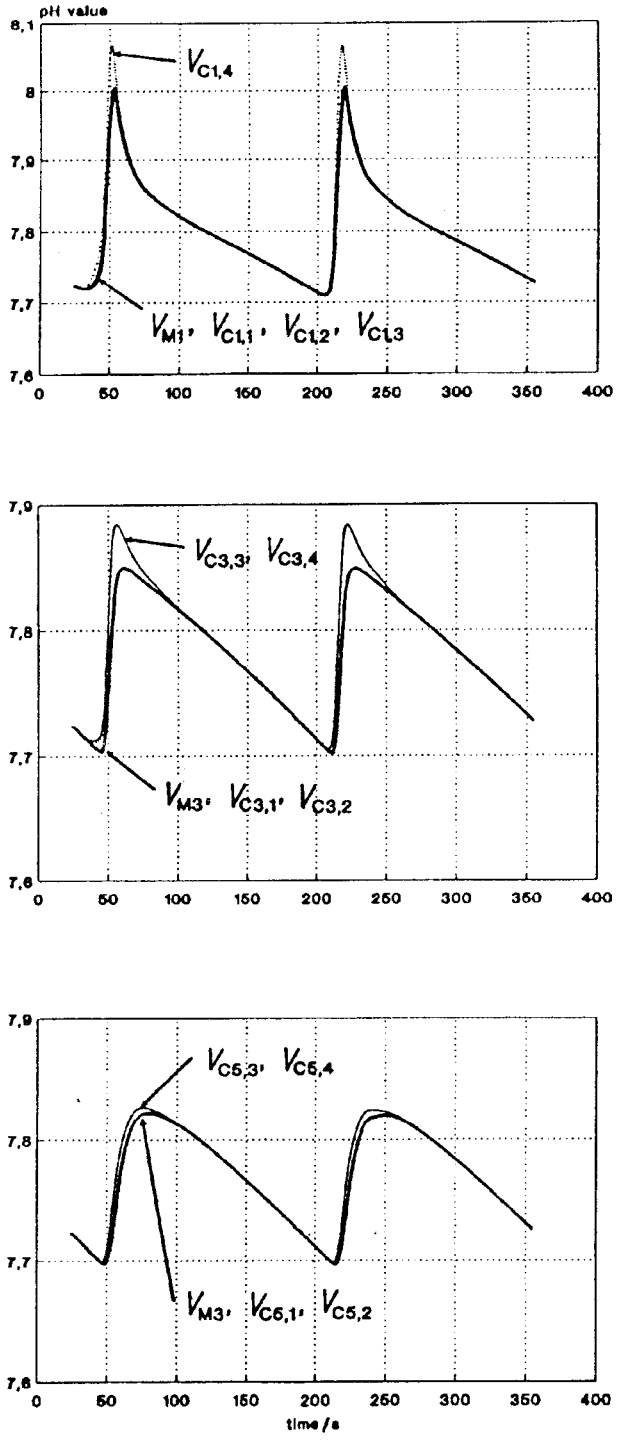

Fig. 15 – *pH time course at different cascades in STR-3-M bioreactor model, the symbols are related to Fig. 4.*
Model parameters:
$t_{c,RAD}$=1.67 s, $t_{c,AX}$=10 s, N_t=4,
V_M/V_{tot}=0.2
pH control parameters:
Q_{NH_3}=0.04 l s^{-1}, P=9.4 g l^{-1}

The pump is switched on at pH=7.7 and switched off if the pH value reaches 7.8 in the compartment of the sensor. In the figure the course of the pH-value is shown for all ideally mixed volumes in three circulation cascades, namely for the first, third and fifth loop (counted from the top). The axial exchange flow is assigned to the third cascade element, therefore the pulse appears stronger in the volume elements before the axial exchange happens. In the top cascade the pulse causes the strongest response, in the lower cascades the pulse is diluted more and more. It becomes clear that the value of the pH changes strongly during the process, although the simulation was not done for the beginning of the fermentation, but for about the 10^{th} hour of it. At this time the fermentation broth has already a rather high buffer capacity, because the product concentration equals approximately 9.4 g l^{-1}.

Both, pump capacity (Fig 16) and size of the switch-on and -off intervall (Fig. 17) have a strong effect on the amplitude of the pH-value. In Fig. 16 the pH-course is illustrated for the top and the middle ideally mixed stirrer compartment. The amplitude is decreased if

– the pumping flow rate of the pump is lowered,

– the interval of the switch is refined.

However, the minimum pumping flow rate is determined by the producivity since all products formed during the fermentation to be neutralized immediately after their production. In our case the minimum flow rate of NH_4OH was about 0.003 l s^{-1}. At the beginning of the fermentation hardly any product

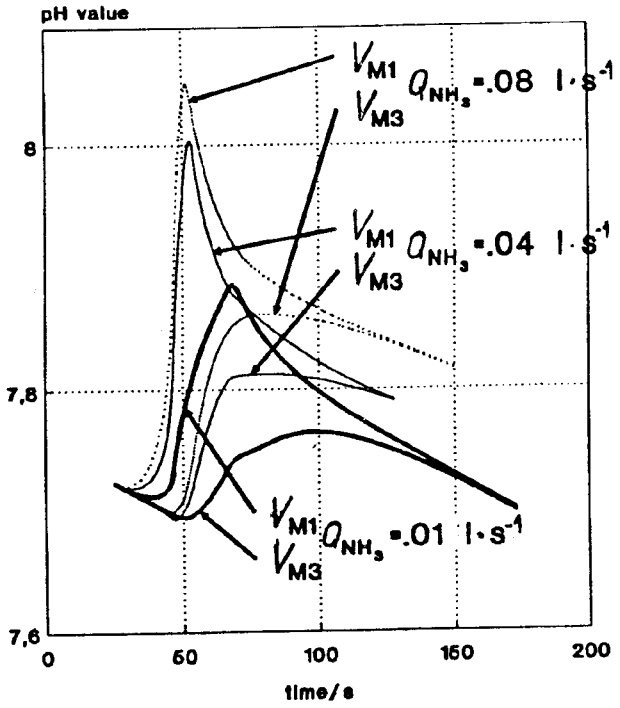

Fig. 16 – *Influence of the pumping capacity of the NH_4OH feed pump on the pH fluctuations. Model parameters are identical to Fig. 15, C_P=9.4 g l^{-1}*

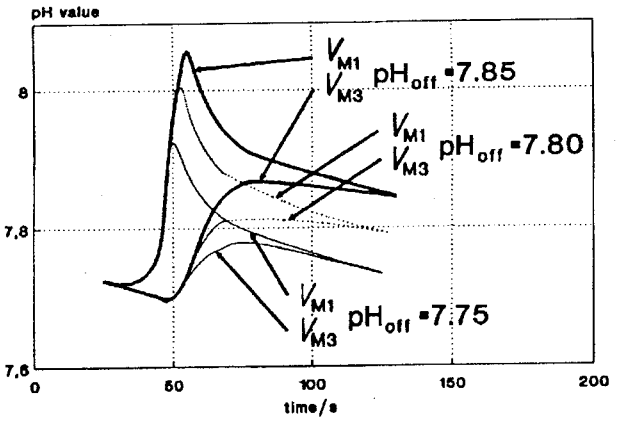

Fig. 17 – *Influence of the sensitivity of the pH sensor on the pH fluctuations. Model parameters and pH control parameters are identical to Fig. 15*

(0.007 g l^{-1}) exists and consequently the buffer capacity is very low. For this reason the amplitude is large (solid line) at the beginning of the experiment compared to the amplitude in case of 9.4 g l^{-1} product (dotted line). At the above calculation only the buffer capacity of the product has been taken into account for the determination of the pH-value. By using a separate buffer in the fermentation broth the amplitude of the pH-fluctuations could be reduced at the beginning of the fermentation, this effect could also be incorporated in the computations.

Anyhow, although the mixing is quite fast a insufficient pH regulation method can cause unexpected large pH fluctuations in the fermentor, which could result in essential problems for the fermentation process. In real fermentations ammoniac can be instroduced as a steam, but this kind of neutralization does not change basically the very precise requirements for the regulation of the amount.

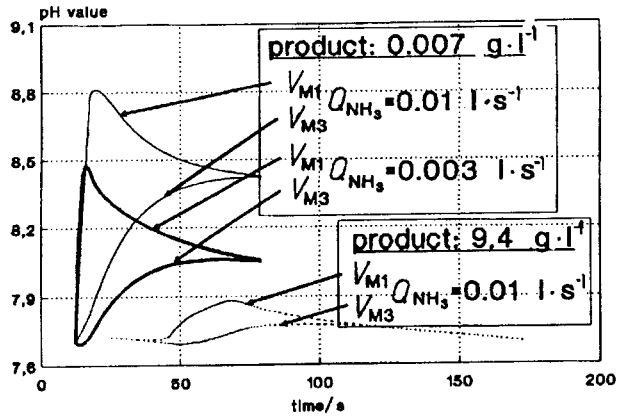

Fig. 18 – *Effect of fermentation time (or amount of product, buffer value) and feed pump capacity on the pH fluctuations. Model parameters: $t_{c,RAD}$=2.78 s, $t_{c,AX}$=2.0 s, N_t=4, V_M/V_{tot}=0.2*

Conclusion

A physical mixing model on basis the tanks-in-series approach was developed and tested for batch stirred tank fermentors. It was utilized in a new scale-up concept which was able to describe the mixing behaviour of 3-stage stirred tank bioreactors from laboratory size up to 65 m^3, including a wide operational range in respect to stirrer revolutions, viscosity and aeration. The four adjustable model parameters, i.e. radial and axial circulation time, ratio of ideally mixed stirrer volume to total liquid volume and the number of compartments in the recirculation cascades, were identified for about 400 experiments by use of modified Monte-Carlo parameter estimation procedure. The stimulated curves fit the experimental data very well, thus proving the adequacy of the chosen mixing model.

The mathematical mixing model was combined with a kinetic model, namely the production of glutamic acid from sugar by *Brevibacterium* sp. The process needed a continuous dosage of base during the fermentation in order to keep the pH-value constant. With the integrated structured bioprocess model, including mixing and kinetics, the pH-value was simulated for different regulation conditions. It became clear that a coarse control of the dosage of base can cause significant negative effects on the bioprocess, especially at the beginning of the fermentation.

ACKNOWLEDGEMENT

This work was kindly supported by the Austrian "Ministerium für Wissenschaft und Forschung" within the Project B12 "Bioreaktoren und Bioprozesse".

List of Symbols

$a_{00} \dots a_{XY}$	–	coefficients in eq. (5)
a_P	$l\,g^{-1}\,s^{-1}$	rate constant
$b_{00} \dots b_{XY}$	–	coefficients in eq. (13)
$c_{P,P}$	$kJ\,kg^{-1}\,K^{-1}$	heat capacity of pulse medium
$c_{P,S}$	$kJ\,kg^{-1}\,K^{-1}$	heat capacity of reactor medium
c_P	$g\,l^{-1}$	product
c_S	$g\,l^{-1}$	substrate
c_X	$g\,l^{-1}$	biomass
d_i	m	stirrer diameter
d_t	m	tank diameter
g	$m\,s^{-2}$	acceleration of gravity
h_l	m	height of fluid in the tank
$i(t)$	–	inhomogeneity-curve
K_S	$g\,l^{-1}$	Monod constant for substrate
K_P	$g\,l^{-1}$	inhibition constant for product
$M(t)$	°C	ideal response curve
n	s^{-1}	stirrer revolutions
N_k	–	number of sensors
N_t	–	number of tanks in the tanks-of-series-cascade
N_P	–	number of measured time intervalls
Q_G	$m^3\,s^{-1}$	aeration flow rate
Q_{NH_3}	$m^3\,s^{-1}$	flow rate of NH_3 dosage
Q_P	$m^3\,s^{-1}$	flow rate of pulse input
r_P	$g\,l^{-1}\,s^{-1}$	rate of production
t	s	time
$t_{c,AX}$	s	axial circulation time
$t_{c,RAD}$	s	radial circulation time
t_{PS}	s	start time of tracer injection
t_{PE}	s	end time of tracer injection
ΔT	°C	system temperature increase due to pulse injection
T_i	°C	temperature of sensors
T_P	s	pulse temperature
T_S	s	mean system temperature before pulse injection
V_i	m^3	volume of compartment i
V_M	m^3	volume of ideally mixed stirrer compartment
V_S	m^3	tank volume before pulse injection
V_{tot}	m^3	total liquid volume
u_0	$m\,s^{-1}$	superficial gas velocity
Y_{XS}	–	yield coefficient for biomass
Y_{PS}	–	yield coefficient for product

Greek:

λ	–	scale ratio ($\lambda = d_{t1}/d_{t,ref}$; $d_{t,ref} = 1.18$ m)
ρ	$kg\,m^{-3}$	density
ρ_P	$kg\,m^{-3}$	density of the pulse medium
ρ_S	$kg\,m^{-3}$	density of the tank medium
η	$Pa \cdot s$	dynamic viscosity
μ	s^{-1}	specific growth rate
μ_{max}	s^{-1}	maximal specific growth rate

Indices:

calc	calculated
m	measured
sim	simulated

Dimensionless numbers:

$$Fr_S = n \cdot \sqrt{\frac{d_i}{g}}$$ stirrer Froude number

$$Fr_A = \frac{u_0}{\sqrt{g \cdot h_l}} = \frac{Q_G}{V_{tot}} \cdot \sqrt{\frac{h_l}{g}}$$ aeration Froude number

References

1. *Moser A.*, Bioprocess Technology, Springer Verlag, New York, Wien, 1988
2. *Reuss M., Bajpai R.*, Stirred tank models, in, *Rehm H.J., Reed G., Pühler A., Stadler P.* (Eds.): Biotechnology, *Schügerl K.* (Volume Ed.): Measuring, modelling and control, Vol. 4, Weinheim, New York, Basel, Cambridge, VCH Verlagsgesellschaft, 1991

3. *Oosterhuis N.M.G.*, Scale-Up of Bioreactors - a Scale-Down Approach, Ph.D.Thesis, Delft University of Technology, 1984
4. *Jury W.*, Mixing in bioreactors, Ph.D.Thesis, Institute for Biotechnology, Graz University of Technology, 1989
5. *Schneider G., Purgstaller A., Somitsch H., Moser A.*, Approach to mixing in bioreactors-experimental verification, methodology and model bioreactor, in *Chmiel H.* et al. (Eds.), Bichemical Engineering, pp 428–430 G. Fischer Verlag, Stuttgart, New York, 1987
6. *Mayr B., Horvat P., Moser A.*, Engineering approach to mixing quantification in bioreactors, accepted (10.12.1991) in Biopr. Eng.
7. *Jury W., Schneider G., Moser A.*, Modelling approach to industrial bioreactors, in 6th european conference on mixing, Pavia, Italy, organized by AIDIC (1988) 451
8. *Levenspiel O.*, Chemical Reactor Omnibook, OSU Book Stores Inc., Corvallis OR, 1979
9. *Mayr B.*, Mixing and Scale-Up of Bioreactors. Measurement and new Quantification Methods, Ph.D Thesis, Institute for Biotehnology, Graz University of Technology, 1992
10. *Schneider G.*, Charakterisierung des Mischungsverhaltens industrieller Rührkesselfermentoren, Ph.D. Thesis in work, Institute for Biotechnology, Graz University of Technology, 1992
11. *Kawase Y., Moo-Young M.*, J.Chem.Tech.Biotechnol. **44** (1989) 63
12. *Mayr B., Horvat P., Nagy E., Moser A.*, Mixing-Models applied to Industrial Batch Bioreactors, accepted (11.5.1992) in Biopr. Eng.
13. *Moser A., Mayr B., Jury W., Steiner W., Horvat P.*, Biopr. Eng. **7** (1991) 171
14. *Moser A., Mayr B., Jury W., Steiner W., Horvat P.*, Biopr. Eng. 7 (1991) 177
15. *Garrison C.M.*, Chem.Eng. (1983) 63
16. *Mayr B., Nagy E., Moser A.*, Scale-Up on basis of structured mixing models. A new concept, in preparation for Biopr.Eng.
17. *Oosterhuis N.M.G., Kossen N.W.F.*, Modeling and Scaling-Up of Bioreactors, in *Brauer H.*: Fundamentals of biochemical engineering, Biotechnology (Vol.2) pp 571–605, Deerfield Beach FL VCH Weinheim, 1985
18. *Singh V., Hensler W., Fuchs R.*, Online Determination of Mixing Parameters in Fermentors Using pH Transient, in Bioreactor Fluid Dynamics, Paper 18, pp 231–256, Cambridge, 1986
19. *Singh V., Fuchs R., Constantinides A.*, A New Method for Fermentor Scale-Up Incorporating both Mixing and Mass Transfer Effects - I. Theoretical Basis, in *Ho C.S., Oldshue J.Y.*, (Eds.); Biotechnology Processes, Scale-Up and Mixing, pp 200–214, AIChE Publ., New York, 1987
20. *Singh V., Fuchs R., Constantinides A.*, Use of Mass Transfer and Mixing Correlation for the Modelling of Oxygen Transfer in Stirred Tank Fermentors, in Bioreactor Fluid Dynamics, Proc.2nd Int. Conf. Cranfield, UK, (1988) 95–115
21. *Bader F.G.*, Biotechnol. Bioeng. **30** (1987) 37–51
22. *Bader F.G.*, Improvements in Multiturbine Mass Transfer Models, in *Ho C.S., Oldsgue J.Y.*, (Eds.); Biotechnology Processes, Scale-Up and Mixing, pp 96–106, AIChE Publ. New York, 1987
23. *Bajpai R.K., Sohn P.U.*, Stage Models for Mixing in Stirred Bioreactors, in *Ho C.S., Oldshue J.Y.*, (Eds.), Biotechnology Processes, Scale-Up and Mixing, pp 13–21 AIChE Publ., New York, 1987
24. *Heinzle E., Kaufmann T., Griot M.*, Modelling of Kinetics, Mass Transfer and Mixing, in *Fish N.M., Fox R.I., Thornhill N.F.* (Eds.), Computer application in fermentation technology, pp 105–109, Elsevier Applied Science, New York, London, 1989
25. *Valko P., Vajda S.*, Solution of Chemical Problems by Personal Computer (in hungarian), Muszaki Konyvkiado, Budapest, 1987
26. *Nakayama K.*, Amino Acids, in Prescott (Ed.), Industrial Microbiology, 4th Edition (1982)
27. *Moser A.*, Biotechn. Bioeng. **37** (1991) 1054
28. *Wenge F., Zuofu L.*, Eng.Chem.Metallurgy **9** (1988) 58
29. *Kishimoto M., Yoshida T., Taguchi H.*, J.Ferm.Techn. **59** (1981) 125